Versatile Immunosensor Using a Quantum Dot Coated Silica Nanosphere as a Label for Signal Amplification

ARTICLE *in* ANALYTICAL CHEMISTRY · AUGUST 2010

Impact Factor: 5.64 · DOI: 10.1021/ac100558t · Source: PubMed

4 AUTHORS, INCLUDING:

Jing Qian
Jiangsu University
53 PUBLICATIONS **544** CITATIONS
SEE PROFILE

X.D. Cao
Hefei University of Technology
17 PUBLICATIONS **364** CITATIONS
SEE PROFILE

Songqin Liu
Anhui
145 PUBLICATIONS **4,214** CITATIONS
SEE PROFILE

Anal. Chem. **2010,** *82,* 6422–6429

Versatile Immunosensor Using a Quantum Dot Coated Silica Nanosphere as a Label for Signal Amplification

Jing Qian, Chunyan Zhang, Xiaodong Cao, and Songqin Liu*

State Key Laboratory of Bioelectronics, School of Chemistry and Chemical Engineering, Southeast University, Nanjing, 211189, People's Republic of China

A versatile immunosensor using a CdTe quantum dots (QDs) coated silica nanosphere (Si/QD) as a label was proposed for ultrasensitive detection of a biomarker. In this approach, silica nanospheres with good monodispersity and uniform structure were employed as the carrier for immobilization of QDs and antibodies. Rabit IgG served as a model protein to demonstrate the performance of the immunosensor. Goat antirabbit IgG antibody was covalently bound to CdTe QDs on the surface of silica nanospheres. CdTe QDs coated with a silica nanosphere label (Si/QD/Ab2) were attached onto the gold electrode surface through a subsequent "sandwich" immunoreaction. This reaction was confirmed by scanning electron microscopic (SEM) and fluorescence microscopic images. Due to signal amplification from the high loading of CdTe QDs, 6.6- and 5.9-fold enhancements in electrochemiluminescent (ECL) and square-wave voltammetric (SWV) signals for IgG detection were achieved compared to the unamplified method. The detection limits for IgG were 1.3 and 0.6 pg mL^{-1} for ECL and SWV measurements, respectively. The resulting versatile immunosensor possesses high sensitivity, satisfactory reproducibility and regeneration, and good precision. This simple and specific strategy has vast potential to be used in other biological assays.

Immunoassays based on specific molecular recognition of an antigen by its antibody have been widely used for quantitative analysis of protein biomarkers in biological samples for clinical purposes.[1,2] These assays have enabled label-free, simple, and even high-throughput detection of target proteins.[3−7] However, increasing demands for early diagnosis of diseases and understanding of fundamental biological processes involved in disease development and progression are pushing the envelope for sensitive detection of biomarkers, especially at low levels.[8,9] Numerous immunoassays have been developed for the enhancement of detection sensitivity by signal amplification or employment of different detection technologies.[10−13] Successful signal amplification strategies include applying new redox-active probes, coupling amplification-by-polymerization concepts with electrochemical detection, integrating enzyme-assisted signal amplification processes, and incorporating nanomaterials to increase loading of tags, etc.[14−20] Among these strategies, the nanoparticle-based amplification has attracted special interests due to the outstanding optical, electronic, and biocompatible performance of nanoparticles. For example, amplification of electrochemical impedance or capacitance signals have been demonstrated in a model fluorescein/antifluorescein system with gold nanoparticles.[21] With the coating of gold nanoparticles on submicrometer-sized latex spheres, the number of Au atoms delivered per sphere was twice as much as reported previously.[22] This advantage made the resultant Au−latex useful as a label for detecting DNA hybridization with a detection limit as low as 0.5 fM.[23] Wang and co-workers reported a novel electrochemical immunoassay strategy using poly(guanine)-functionalized silica nanoparticles as a label.[24−26] The detection signal, anodic current of catalytic

* To whom correspondence should be addressed. E-mail: liusq@seu.edu.cn. Phone: +86-25-52090613. Fax: +86-25-52090618.

(1) Gambhir, S. S. *Nat. Rev. Cancer* **2002**, *2*, 683–693.
(2) Wilson, M. S.; Nie, W. Y. *Anal. Chem.* **2006**, *78*, 6476–6483.
(3) Jie, G. F.; Liu, B.; Pan, H. C.; Zhu, J. J.; Chen, H. Y. *Anal. Chem.* **2007**, *79*, 5574–5581.
(4) Zhong, Z. Y.; Li, M. X.; Xiang, D. B.; Dai, N.; Qing, Y.; Wang, D.; Tang, D. P. *Biosen. Bioelectron.* **2009**, *24*, 2246–2249.
(5) Ho, D.; Falter, K.; Severin, P.; Gaub, H. E. *Anal. Chem.* **2009**, *81*, 3159–3164.
(6) Parker, C. O.; Lanyon, Y. H.; Manning, M.; Arrigan, D. W. M.; Tothill, I. E. *Anal. Chem.* **2009**, *81*, 5291–5298.
(7) Yang, R. H.; Tang, Z. W.; Yan, J. L.; Kang, H. Z.; Kim, Y.; Zhu, Z.; Tan, W. H. *Anal. Chem.* **2008**, *80*, 7408–7413.
(8) Teppo, A. M.; Maury, C. P. J. *Clin. Chem.* **1987**, *33*, 2024–2027.
(9) Deiss, F.; LaFratta, C. N.; Symer, M.; Blicharz, T. M.; Sojic, N.; Walt, D. R. *J. Am. Chem. Soc.* **2009**, *131*, 6088–6089.
(10) Takeuchi, T.; Matile, S. *J. Am. Chem. Soc.* **2009**, *131*, 18048–18049.
(11) Lai, G. S.; Yan, F.; Ju, H. X. *Anal. Chem.* **2009**, *81*, 9730–9736.
(12) Nam, J. M.; Thaxton, C. S.; Mirkin, C. A. *Science* **2003**, *301*, 1884–1886.
(13) Wu, Y. F.; Liu, S. Q.; He, L. *Anal. Chem.* **2009**, *81*, 7015–7021.
(14) Chen, Z. P.; Peng, Z. F.; Luo, Y.; Qu, B.; Jiang, J. H.; Zhang, X. B.; Shen, G. L.; Yu, R. Q. *Biosen. Bioelectron.* **2007**, *23*, 485–491.
(15) Tang, D. P.; Ren, J. J. *Anal. Chem.* **2008**, *80*, 8064–8070.
(16) Wang, J.; Meng, W. Y.; Zheng, X. F.; Liu, S. L.; Li, G. X. *Biosen. Bioelectron.* **2009**, *24*, 1598–1602.
(17) Zhang, S. S.; Zhong, H.; Ding, C. F. *Anal. Chem.* **2008**, *80*, 7206–7212.
(18) Mak, W. C.; Cheung, K. Y.; Trau, D.; Warsinke, A.; Scheller, F.; Renneberg, R. *Anal. Chem.* **2005**, *77*, 2835–2841.
(19) Liao, W.-C.; Ho, J. A. *Anal. Chem.* **2009**, *81*, 2470–2476.
(20) Wang, J.; Li, J. H.; Baca, A. J.; Hu, J. B.; Zhou, F. M.; Yan, W.; Pang, D. W. *Anal. Chem.* **2003**, *75*, 3941–3945.
(21) Wang, J. B.; Profitt, J. A.; Pugia, M. J.; Suni, I. I. *Anal. Chem.* **2006**, *78*, 1769–1773.
(22) Kawde, A. N.; Wang, J. *Electroanalysis* **2004**, *16*, 101–107.
(23) Pinijsuwan, S.; Rijiravanich, P.; Somasundrum, M.; Surareungchai, W. *Anal. Chem.* **2008**, *80*, 6779–67840.
(24) Wang, J.; Liu, G.; Engelhard, M. H.; Lin, Y. *Anal. Chem.* **2006**, *78*, 6974–6979.

10.1021/ac100558t
Published on Web 07/02/2010

oxidation of guanine in the presence of $Ru(bpy)_3^{2+}$, was amplified by an increase in guanine residues trapped on the electrode surface with poly(guanine)-functionalized silica nanoparticle labels. Our previous study demonstrated that the signal amplification could also be achieved by using enzyme-functionalized silica nanoparticle as an immunological label. A 29.5- and 61-fold increase of detection signal was observed in electrochemical and chemiluminescence measurements, respectively, compared with the traditional sandwich immunoassay.[27] These examples indicate nanoparticles are excellent carriers in the transduction amplification of recognition events.

Semiconductor quantum dots (QDs) are other popular kinds of nanostructured materials used for constructing biosensors due to their numerous advantageous features, such as broad excitation spectra for multicolor imaging, robust and narrowband emissions, and feasibility for surface modification.[28−33] They have been used as electrochemiluminescence (ECL) and luminescence labels for bioassays and bioimagings.[34−38] For example, Cui et al.[39] recently developed a versatile sandwich-type immunosensor using CdTe QDs as labels. The sensor was fabricated on an indium−tin oxide chip covered with a well-ordered gold nanoparticle monolayer. On the basis of gel imaging system, Cui et al. could simultaneously detect samples with a series of different concentrations of a target analyte. This paved a way to develop a rapid and highly specific method for sensitive detection of biological substances. However, the occurrence of agglomeration during the cross-linking reaction made direct bioconjugation of these QDs with biomolecules difficult, which influenced the stability, precision, and reproducibility of the resultant immunosensors.

More recently, we prepared an electrochemical immunsensor based on a CdTe QDs functionalized silica nanosphere label for protein detection. Silica nanoparticles with good monodispersity were employed as carriers for immobilization of QDs and antibodies. α-Fetoprotein (AFP) antibody was covalently bound to CdTe QDs on the surface of silica nanoparticles. Enhanced sensitivity could be achieved by an increase of CdTe QD loading per sandwich immunoreaction.[40] To further expand this strategy for other protein detections with different detection technologies, we present herein a detailed investigation on synthetic strategy of CdTe QDs coated silica nanosphere (Si/QD) labels and their versatile applications in immunoassays. To obtain immunosensors with good regenerative performance, a poly(*o*-aminobenzoic acid) (PAB) film was constructed on gold surface for the immobilization of goat antirabbit IgG antibodies. The Si/QD labels were brought to the gold electrode surface through a subsequent "sandwich" immunoreaction, which allowed sensitive detection of IgG antibodies, with detection limits of 1.3 and 0.6 pg mL^{-1} for ECL and SWV measurements, respectively.

EXPERIMENTAL SECTION

Reagents. Goat antirabbit IgG antibody (Ab, 10 mg mL^{-1}) and rabbit IgG antigen (Ag, 33.3 mg mL^{-1}) were obtained from Signalway Antibody Co. (Nanjing, China). Carcinoma antigen 199 (CA-199) and carcinoembryonic antigen (CEA) were purchased from Boson Biotech Co. Ltd. (Xiamen, China). 1-Ethyl-3-(3-dimethylaminopropyl) carbodiimide hydrochloride (EDC), *N*-hydroxysuccinimide (NHS), (3-aminopropyl)-triethoxysilane (APTS), and bovine serum albumin (BSA) were purchased from Sigma-Aldrich Chemicals Co. Tetraethoxysilane (TEOS) was obtained from Zhang-Jiakou Guotai-Huarong New Chemical Materials Co. Ltd. (Zhang-Jiakou, China). *o*-Aminobenzoic acid was a gift from Xingshengchem (Yancheng, China). Bismuth nitrate pentahydrate was purchased from Kermel Chemical Reagents Development Centre (Tianjin, China). CdTe QDs, with diameter of 2.77 nm and stabilized with mercaptoacetic acid, were obtained from Shenzhen Biological Tech. Co. (Shenzhen, China). All other chemicals were of analytical grade and were used as received. The 0.1 M phosphate buffer solutions (PBS) were prepared by mixing 0.1 M NaH_2PO_4 and Na_2HPO_4. Twice-distilled water was used throughout the study.

Apparatus. The electrochemical and ECL measurements were carried out on an MPI-E multifunctional electrochemiluminescent analytical system (Xi'an Remex Analyze Instrument Co. Ltd., China). All ECL measurements were performed in a 5 mL glass cell composed of a modified Au working electrode, a platinum counter electrode, and a Ag/AgCl (saturated KCl solution) reference electrode.

Cyclic voltammetric (CV) and square-wave voltammetric (SWV) measurements were performed with a CHI 832B electrochemical workstation (CH Instrument Co. Shanghai). A conventional three-electrode system consisted of a modified bismuth film modified glassy carbon electrode (BFE), a platinum wire, and a saturated calomel electrode (SCE) as the working, auxiliary, and reference electrodes in electrochemical measurements, respectively.

The morphology and size of silica and CdTe QDs coated silica nanoparticles (Si/QD) were analyzed with a transmission electron microscope (TEM, S-2400N, HITACHI, Japan). The goat antirabbit IgG antibody (Ab2)-modified Si/QD (Si/QD/Ab2) was attached to the goat antirabbit IgG antibody (Ab1)-modified Au substrate through a sandwich immunoassay process. The reaction was confirmed by a scanning electron microscope (SEM, JEM-2100, JEOL, Japan) at an acceleration voltage of 30 kV, and fluorescence microscopy images were carried out with an Olympus IX71 Inverted Optical Microscope (Olympus, Japan). Photoluminescence (PL) spectra were obtained on an RF-540 spectrophotometer (Shimadzu, Japan). UV−vis spectra were performed with a UV-2450 spectrophotometer (Shimadzu, Japan). X-ray photoelectron

(25) Wang, J.; Liu, G.; Wu, H.; Lin, Y. *Anal. Chim. Acta* **2008**, *610*, 112–118.
(26) Wang, J.; Liu, G.; Lin, Y. *Small* **2006**, *2*, 1134–1138.
(27) Wu, Y. F.; Chen, C. L.; Liu, S. Q. *Anal. Chem.* **2009**, *81*, 1600–1607.
(28) Myung, N.; Ding, Z. F.; Bard, A. J. *Nano Lett.* **2002**, *2*, 1315–1319.
(29) Green, M. *Angew. Chem., Int. Ed.* **2004**, *43*, 4129–4131.
(30) Klostranec, J. M.; Chan, W. C. W. *Adv. Mater.* **2006**, *18*, 1953–1964.
(31) Goldman, E. R.; Balighian, E. D.; Mattoussi, H.; Kuno, M. K.; Mauro, J. M.; Tran, P. T.; Anderson, G. P. *J. Am. Chem. Soc.* **2002**, *124*, 6378–6382.
(32) Mattoussi, H.; Mauro, J. M.; Goldman, E. R.; Anderson, G. P.; Sundar, V. C.; Mikulec, F. V.; Bawendi, M. G. *J. Am. Chem. Soc.* **2000**, *122*, 12142–12150.
(33) Zou, Z. X.; Du, D.; Wang, J.; Smith, J. N.; Timchalk, C.; Li, Y. Q.; Lin, Y. H. *Anal. Chem.* **2010**, *82*, 5125–5133.
(34) Hu, X. F.; Wang, R. Y.; Ding, Y.; Zhang, X. L.; Jin, W. R. *Talanta* **2010**, *80*, 1737–1743.
(35) Carroll-Portillo, A.; Bachand, M.; Greene, A. C.; Bachand, G. D. *Small* **2009**, *5*, 1835–1840.
(36) Li, J.; Zhao, X. W.; Zhao, Y. J.; Gu, Z. Z. *Chem. Commun.* **2009**, *17*, 2329–2331.
(37) Wang, Q.; Kuo, Y. C.; Wang, Y. W.; Shin, G.; Ruengruglikit, C.; Huang, Q. R. *J. Phys. Chem. B* **2006**, *110*, 16860–16866.
(38) Wang, J.; Liu, G. D.; Wu, H.; Lin, Y. H. *Small* **2008**, *4*, 82–86.
(39) Cui, R. J.; Pan, H. C.; Zhu, J. J.; Chen, H. Y. *Anal. Chem.* **2007**, *79*, 8494–8501.
(40) Chen, L. Y.; Chen, C. L.; Li, R. N.; Li, Y.; Liu, S. Q. *Chem. Commun.* **2009**, *19*, 2670–2672.

spectroscopy (XPS, ESCALAB 250 multitechnique surface analysis system, Thermo Electron Co., U.S.A.) was used to probe the binding nature of Ab2 with CdTe QDs capped silica nanoparticle. The statistical distribution of the relative emission intensities, corresponding to green along the white lines, was extracted using a self-developed software. This system was able to count pels, referring to a certain color of a photo.

Preparation of the Si/QD/Ab2 Labels. Monodispersed silica nanoparticles, used as carriers for QDs and Ab2 immobilization, were synthesized with our previously reported seed-growth method.[27,40,41] The diameter of the as-prepared silica nanoparticles was 100 ± 3.0 nm, determined by TEM microscopy.

Preparation of CdTe QDs Coated Silica Nanoparticles (Si/QD). For the preparation of CdTe QDs coated silica nanoparticles, 0.02 g of silica nanospheres was first dispersed in 2 mL of ethanol and treated with 0.4 mL of APTS. After stirring for 6 h, the suspension was centrifuged and washed with ethanol repeatedly for four times, and the amino-functionalized nanoparticles were obtained. Then, the amino-functionalized silica nanoparticles were dispersed in a mixture of 1 mL of CdTe QDs (5 mg mL^{-1}) stabilized with 3-mercaptopropionic acid and 1 mL of EDC (20 mg mL^{-1}). The mixed suspension was stirred at 4 °C for 12 h. Unbound QDs were removed by successive centrifugation and washing with water several times. Finally, the as-prepared Si/QD nanospheres, which had the same orange color as CdTe QDs itself, were obtained and dispersed in water to a final volume of 1 mL.

Preparation of QDs Coated Silica Nanosphere Immunological Labels (Si/QD/Ab2). To generate QDs-coated silica nanosphere immunological labels, 1 mL of the above Si/QD suspension was mixed with 1 mL of Ab2 solution (anti-IgG, 20 μg mL^{-1}, in 0.01 M pH 7.4 PBS). Subsequently, 100 μL of freshly prepared EDC (20 mg mL^{-1}, in 0.1 M pH 7.4 PBS) and 100 μL of NHS (10 mg mL^{-1}, in 0.1 M pH 7.4 PBS) were added. After incubation at room temperature for 2 h, free antibody was removed by centrifugation and washing with 0.01 M PBS for several times to obtain the Ab2-modified Si/QD nanoparticles (Si/QD/Ab2). Finally, Si/QD/Ab2 nanoparticles were redispersed in 5 mL of 1% BSA solution for 2 h, again under stirring, to block the excess amino group and nonspecific binding sites of the Si/QD/Ab2 nanospheres. After being centrifuged and washed with PBS, the resultant Si/QD/Ab2 nanoparticles were dispersed with 0.01 M of pH 7.4 PBS to a final volume of 2 mL and stored at 4 °C for later use. The whole process for construction of Si/QD/Ab2 labels is illustrated in Scheme 1.

Preparation of the Anti-IgG-Modified Au Substrates. The preparation of the anti-IgG-modified Au substrates is illustrated in Scheme 2. Prior to each measurement, Au substrates were polished with polishing cloths and alumina powder down to 0.05 μm, followed by successive sonication in water and ethanol. Electrodes were then rinsed with twice-distilled water and soaked in freshly prepared piranha solution for 1 h (safety note: the piranha solution should be handled with extreme caution). For anti-IgG immobilization, a poly(*o*-ABA) (PAB) film was electropolymerized on the gold electrode surface. Briefly, a clean electrode was dipped in a 1 M H_2SO_4 solution containing 50 mM *o*-ABA and scanned in a potential range of 0−1.0 V for 10 cycles at a scan rate of 40 mV s^{-1}.[42,43] The PAB-modified electrodes were then removed from the solution, rinsed with water three times, immersed in water for 30 min and then in 200 μL of EDC/NHS solution (20 mg mL^{-1} EDC and 10 mg mL^{-1} NHS in 0.1 M pH 7.4 PBS) for another 30 min. After washing thoroughly with water, 10 μL of anti-IgG (100 μg L^{-1}, in 0.01 M pH 7.4 PBS, denoted Ab1) was dropped onto the surface of PAB-modified Au substrates. After 12 h of incubation at 4 °C, the electrode was washed thoroughly with PBS and then soaked in 1% BSA solution at 4 °C for 30 min to block the nonspecific binding sites on the electrode surface. The final product was an anti-IgG-modified Au electrode (Ab1−PAB−Au).

Scheme 1. Preparation of Si/QD/Ab2[a]

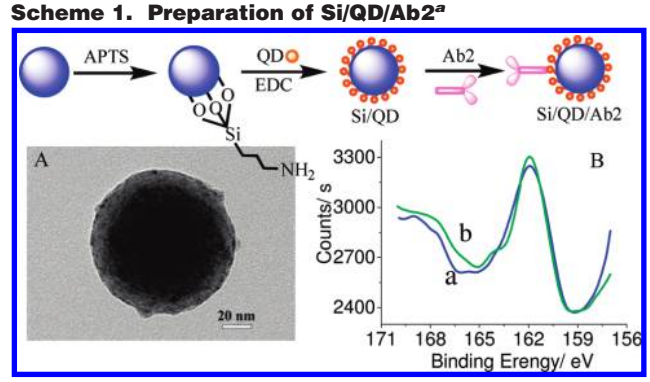

[a] Inset A represents the TEM images of the as-synthesized Si/QD; inset B is the XPS of S 2p of (a) Si/QD and (b) Si/QD/Ab2 nanoparticles.

Scheme 2. Schematic Diagram of the Sandwich Immunoassay with Si/QD/Ab2 as a Label[a]

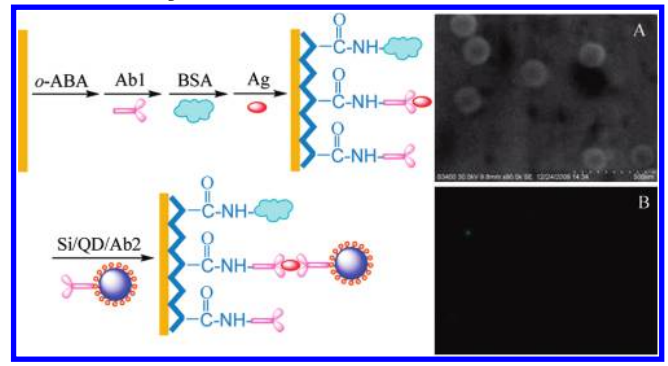

[a] Insets: (A) SEM and (B) fluorescence microscopic images of Ab1−PAB-modified Au substrate exposed to the 5 ng mL^{-1} IgG solution, followed by Si/QD/Ab2 suspension. The excited wavelength is 488 nm.

Sandwich Immunoassay with Si/QD/Ab2 as the Label. A sandwich immunoassay procedure using Si/QD/Ab2 as label is shown in Scheme 2. The Ab1−PAB−Au was incubated in 100 μL of IgG solution at 37 °C for 40 min to capture Ag with the first immunoreaction (Ag−Ab1−PAB−Au). After washing thoroughly with PBS, the Ag−Ab1−PAB−Au was exposed to 0.5 mL of Si/QD/Ab2 suspension. In order to introduce Si/QD/Ab2 onto the electrode surface through the second immunoreaction, the electrode was immersed in the mixture and stirred for 40 min at room temperature (25 ± 1 °C). Then it was thoroughly rinsed with PBS to remove the physical adsorption of Si/QD/Ab2. This

(41) Chen, C. L.; Li, Y.; Liu, S. Q. *J. Electroanal. Chem.* **2009**, *632*, 14–19.
(42) Preechaworapun, A.; Dai, Z.; Xiang, Y.; Chailapakul, O.; Wang, J. *Talanta* **2008**, *76*, 424–431.
(43) Wang, Y. J.; Knoll, W. *Anal. Chim. Acta* **2006**, *558*, 150–157.

completed a sandwich immunoassay, and the Si/QD/Ab2-modified Au electrode (Si/QD/Ab2−Ag−Ab1−PAB−Au) were thus obtained.

Fabrication of Bismuth Film Modified Glassy Carbon Electrode. The glassy carbon electrode (GC) (3 mm diameter) was polished before each experiment with 1.0 and 0.3 μm α-alumina slurry. It was also rinsed thoroughly with twice-distilled water between each polishing step, followed by successive sonication in water and ethanol. The bismuth film modified GC electrode (BFE) was fabricated by dipping the GC electrode in a bismuth nitrate solution in acetate with a final pH of 2.0 and Bi(III) ion concentration of 1.25 mg mL^{-1} and applied a potential of −1.0 V (vs SCE) for 120 s.

ECL Detection. The ECL measurements were performed in a 5 mL glass cell. The electrolyte was a 0.1 M pH 7.4 PBS containing 0.1 M KCl and 0.1 M $K_2S_2O_8$. The potential range applied to the Au disk working electrode (2 mm diameter) in the CV measurement was from 0 to −1.7 V at 100 mV s^{-1}. The ECL emission intensity (I_{ECL}) corresponding to CV measurements was recorded by the MPI-E multifunctional electrochemiluminescence analyzer at room temperature. The emission window was placed in front of the photomultiplier tube, which was biased at 1000 V.

SWV Analysis. Si/QD/Ab2−Ag−Ab1−PAB−Au was immersed in 200 μL of 0.1 M glycine−HCl (pH 2.2) solution for 10 min. Then it was washed by 0.1 M PBS for three times and diluted with 0.1 M pH 7.0 PBS to a final volume of 3 mL. The analytical procedure involved 120 s of electrodeposition at −1.2 V for three times (10 s stirring was applied between each accumulation period). After that, it was stripped by scanning from −1.3 to −0.5 V using SWV measurements with 4 mV potential steps, 15 Hz frequency, and 25 mV amplitude.

RESULTS AND DISCUSSION

Synthesis of Si/QD/Ab2 Labels. Silica nanoparticles with good monodispersion and similar surface morphology were vital to consistent loading of QDs and antibody on each nanosphere, as they influence the sensitivity, reproducibility, and analytical performance of the resultant immunosensor. In this specific case, the silica nanospheres were synthesized with our previously reported seed-growth method.[27,40,41] The TEM images showed that the as-prepared silica nanoparticles had a chemically clean and homogenized structure with a diameter of 100 ± 3.0 nm (see Supporting Information Figure S-1, parts A and B). Coating of the CdTe QDs onto the surface of silica nanospheres was achieved through acylamide binding in the presence of EDC as the activator. As shown in Scheme 1, APTS was first coupled to the hydroxyl group on the surface of silica nanospheres to yield an amino-terminated self-assembled monolayer. Subsequently, the carboxylic groups located on the surface of CdTe QDs were reacted with amino distal points to form QDs-coated silica nanoparticles. Coating of CdTe QDs on silica nanospheres was demontrated by the color change under sunlight and UV illumination (λ_{ex} = 365 nm) (Supporting Information Figure S-2), as well as UV−vis and PL spectra (Supporting Information Figure S-3). After being coated with CdTe QDs, the silica nanospheres showed the same color as CdTe QDs in water. Furthermore, when using 380 nm as λ_{ex}, the resultant nanospheres displayed an absorption peak at 517 nm and a strong PL emission peak at 555 nm, consistent with the CdTe QDs itself. The coating of QDs on silica nanospheres was also confirmed by TEM images (Scheme 1A and Supporting Information Figure S-1C). After the coating process, QDs were deposited on the surface of silica nanospheres, probably in a uniform fashion. All these results confirmed that CdTe QDs had been successfully planted onto the surface of silica nanospheres with excellent dispersivity. Such good dispersivity prevented the particles from agglutination, a common problem that occurs when using small nanoparticles as biological labels.[37]

Table 1. X-ray Photoelectron Spectroscopic Data for Si/QD and Si/QD/Ab2

	elemental composition (%)						
sample	C	Si	O	N	Cd	Te	S
Si/QD	26.68	16.56	42.27	2.51	7.14	2.81	2.03
Si/QD/Ab2	53.40	8.18	22.90	7.60	3.94	1.56	2.42

Mercaptoacetic acid on CdTe QD surface could react with the amino group in the antibody in the presence of EDC and NHS as activating reagents. This reaction would bind the antibody to the QDs. Attachment of antibody did not affect PL emission of QDs coated on the silica nanospheres (Supporting Information Figure S-2B). XPS was used to confirm whether the antibody was attached to the surface of silica nanoparticles. Change of elemental compositions for carbon (C 1s), silicon (Si 2p), oxygen (O 1s), nitrogen (N 1s), cadmium (Cd 3d5), tellurium (Te 3d5), and sulfur (S 2p) before and after being Ab2 coated (without the BSA blocking process) is summarized in Table 1. Coupling of Ab2 on Si/QD resulted in an increase in the relative elemental compositions of carbon, nitrogen, and sulfur and a decrease in the unrelative elemental compositions of silicon, cadmium, and tellurium. In addition, both Si/QD and Si/QD/Ab2 displayed a S 2p peak at 161.9 eV in their high-resolution XPS spectra (Scheme 1B), which could be attributed to Cd−S−R bond.[44] However, after Ab2 coupling, a clear shoulder peak of S 2p located at 164.1 eV was observed. This shoulder peak corresponded to a disulfide bond in protein.[45,46] All these facts confirmed the successful synthesis of the Si/QD/Ab2 label.

Sandwich Immunoassay Using Si/QD/Ab2 as the Label. The sandwich immunoassay process is outlined in Scheme 2. Specifically, PAB film with abundant carboxyl groups was electrodeposited on the gold surface for antibody coupling. Then, the antibody-coated gold electrode was used to capture IgG from the IgG-containing solution through the first immunoreaction. Finally, Si/QD/Ab2 labels were immobilized on the Au surface during the secondary binding event. The insets in Scheme 2, parts A and B, are representative SEM images and fluorescence microscopic (excited at a blue light excitation corresponding to 488 nm) images of the Si/QD/Ab2−Ag−Ab1−PAB−Au at an IgG concentration of 5 ng mL^{-1}, respectively (SEM images of bare Au and PAB−Au, fluorescence microscopy of Ag−Ab1−PAB−Au are

(44) Cheng, L. X.; Liu, X.; Lei, J. P.; Ju, H. X. *Anal. Chem.* **2010**, *82*, 3359–3364.
(45) Chi, Q. J.; Zhang, J. D.; Nielsen, J. U.; Friis, E. P.; Chorkendorff, I.; Canters, G. W.; Andersen, J. E. T.; Ulstrup, J. *J. Am. Chem. Soc.* **2000**, *122*, 4047–4055.
(46) Hansen, A. G.; Boisen, A.; Nielsen, J. U.; Wackerbarth, H.; Chorkendorff, I.; Andersen, J. E. T.; Zhang, J. D.; Ulstrup, J. *Langmuir* **2003**, *19*, 3419–3427.

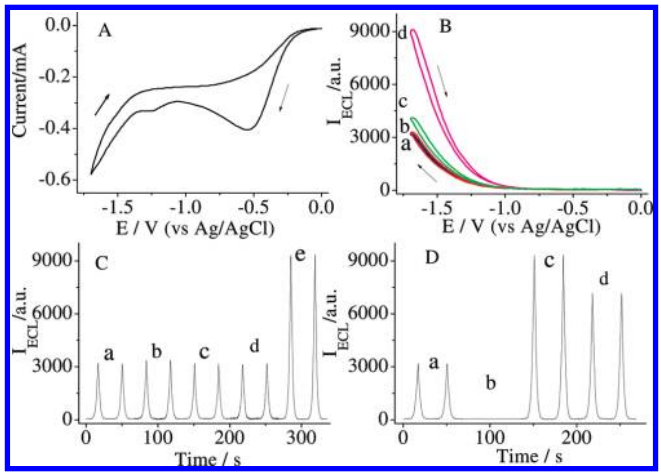

Figure 1. (A) CV of Si/QD/Ab2−Ag−Ab1−PAB−Au at an IgG concentration of 1 ng mL^{-1}. (B) I_{ECL}−E curves obtained at (a) bare Au, Ab1−PAB−Au incubated in 1 ng mL^{-1} IgG solution (b−d), followed in QD/Ab2 (c) and Si/QD/Ab2 (d) suspension. (C) ECL response of Ag−Ab1−PAB−Au at an IgG concentration of 1 ng mL^{-1} (a) and Ab1−PAB−Au incubated in 0 (b), 1 ng mL^{-1} IgG (e), 25 ng mL^{-1} CA-199 (c), 40 ng mL^{-1} CEA (d) for 40 min, followed by Si/QD/Ab2 suspension for 40 min. (D) ECL response of bare Au (a) and Si/QD/Ab2−Ag−Ab1−PAB−Au (b and c) in air-saturated 0.1 M pH 7.4 PBS containing 0.1 M KCl with (a and c) or without (b) the presence of 0.1 M $K_2S_2O_8$; (d) Si/QD/Ab2−Ag−Ab1−PAB−Au in 0.1 M pH 7.4 PBS containing 0.1 M KCl and 0.1 M $K_2S_2O_8$ after removing oxygen with pure nitrogen for 15 min.

shown in Supporting Information Figure S-4). Several particles with diameter of approximately 100 nm are observed in Scheme 2A, while some small green fluorescence spheres are observed in Scheme 2B, indicating that the Si/QD/Ab2 nanospheres were successfully attached to the gold surface through the Ag−Ab interaction. In control experiments, where the Ag−Ab1−PAB−Au surface was incubated in Si/QD suspension without coupling with Ab2, the Ab1−PAB−Au was incubated in Si/QD/Ab2 suspension without prior exposure to the IgG-containing solution, and Ab1−PAB−Au was incubated in 25 ng mL^{-1} CA-199 and 40 ng mL^{-1} CEA, followed by soaking in Si/QD/Ab2 suspension. In these situations, particles were not observed in both the SEM and fluorescence microscopic images (data not shown). All these confirmed the observed particles in both parts A and B of Scheme 2 were from a highly specific immunoreaction and that CdTe QDs on Si/QD/Ab2−Ag−Ab1−PAB−Au were able to keep their fluorescence property.

Signal Amplification Using Si/QD/Ab2 as an ECL Label. The sandwich immunassay using Si/QD/Ab2 as a label was also supported by ECL measurements. Figure 1A shows the CVs of Si/QD/Ab2−Ag−Ab1−PAB−Au at an IgG concentration of 1 ng mL^{-1}, and curve d in Figure 1B is the corresponding ECL signal of the same electrode in air-saturated 0.1 M pH 7.4 PBS containing 0.1 M KCl and 0.1 M $K_2S_2O_8$. The large increase of ECL emission intensity at −1.68 V (vs Ag/AgCl) was observed from Si/QD/Ab2−Ag−Ab1−PAB−Au (Figure 1B, curve d), whereas no obvious increase of ECL emission could be observed from bare gold (Figure 1B, curve a), PAB−Au (data not shown), Ab1−PAB−Au (data not shown), and Ag−Ab1−PAB−Au at an IgG concentration of 1 ng mL^{-1} (Figure 1B, curve b). These results suggested that enhanced ECL emission intensity was attributed to attached Si/QD/Ab2 on the electrode surface, which could react with $S_2O_8^{2-}$ and enhance the ECL signal.

To support this opinion, a series of control experiments were conducted by incubating Ab1−PAB−Au in 0 ng mL^{-1} IgG (Figure 1C, curve b), 25 ng mL^{-1} CA-199 (Figure 1C, curve c), and 40 ng mL^{-1} CEA (Figure 1C, curve d), followed by incubation in Si/QD/Ab2 suspension. The ECL responses showed only minor difference with Ag−Ab1−PAB−Au at IgG concentration of 1 ng mL^{-1} itself (Figure 1C, curve a). However, when Ab1−PAB−Au was incubated in 1 ng mL^{-1} IgG solution, followed by Si/QD/Ab2 suspension (Figure 1C, curve e), the ECL signal of the resultant electrode increased significantly. All these results demonstrated that the QDs label could be loaded to the electrode surface through highly specific sandwich immunoreactions and not originated from physical absorption or cross-reaction; the attached Si/QD/Ab2 effectively retained its ECL properties. These advantages allowed it to be used as a biological label for ECL immunoassay. Furthermore, the ECL intensity of Si/QD/Ab2−Ag−Ab1−PAB−Au was 6.6-fold that of QD/Ab2−Ag−Ab1−PAB−Au (Figure 1B, curve c, CdTe QDs bound directly with Ab2 and used as the label) at the same IgG concentration, which demonstrated the amplification of ECL signal with Si/QD/Ab2 as the label.

To gain a better understanding of the ECL generation, some control experiments were performed, as shown in Figure 1D. Ab2−Ag−Ab1−PAB−Au at IgG concentration of 1 ng mL^{-1} (without CdTe QDs coupling) was tested in a 0.1 M pH 7.4 air-saturated PBS solution containing 0.1 M $K_2S_2O_8$ and 0.1 M KCl. A clear ECL emission was observed (Figure 1D, curve a). This ECL emission could be greatly enhanced in the presence of Si/QD/Ab2 on the electrode surface (Figure 1D, curve c). On the other hand, no ECL emission was observed for Si/QD/Ab2−Ag−Ab1−PAB−Au in a 0.1 M pH 7.4 air-saturated PBS containing 0.1 M KCl without $K_2S_2O_8$ (Figure 1D, curve b). This indicated that $S_2O_8^{2-}$ played a key role in the cathodic ECL. From the CV in Figure 1A, two cathodic peaks at −1.22 and −0.54 V were observed from Si/QD/Ab2−Ag−Ab1−PAB−Au in 0.1 M pH 7.4 air-saturated PBS containing 0.1 M $K_2S_2O_8$ and 0.1 M KCl, respectively. This was in good agreement with the observations for CdS QDs bound directly with protein as label.[3,47] The small peak at −1.22 V was attributed to electrochemical reduction of attached CdTe QDs on the electrode surface, which produced negatively charged radicals of $CdTe^{-\bullet}$. The large reduction peak at −0.54 V was attributed to the reduction of $S_2O_8^{2-}$ to anion sulfate radical $SO_4^{-\bullet}$.[3,34] The product, $SO_4^{-\bullet}$, was then reacted with $CdTe^{-\bullet}$ by injecting a hole into the highest occupied molecular orbital (HOMO) of $CdTe^{-\bullet}$ to obtain an excited state (CdTe*). This state emitted light in the aqueous solution to produce an ECL signal. When dissolved oxygen was removed from the solution by bubbling high-purity nitrogen, the ECL emission was a little lower than that of the air-saturated solution (Figure 1D, curve d). These results agreed with the result that oxygen can be reduced and used to catalyze ECL emission of QDs.[48] Thus, in an air-saturated solution, the following reactions should be involved in the ECL

(47) Jie, G. F.; Huang, H. P.; Sun, X. L.; Zhu, J. J. *Biosen. Bioelectron.* **2008**, *23*, 1896–1899.
(48) Han, H. Y.; Sheng, Z. H.; Lian, J. G. *Anal. Chim. Acta* **2007**, *596*, 73–78.

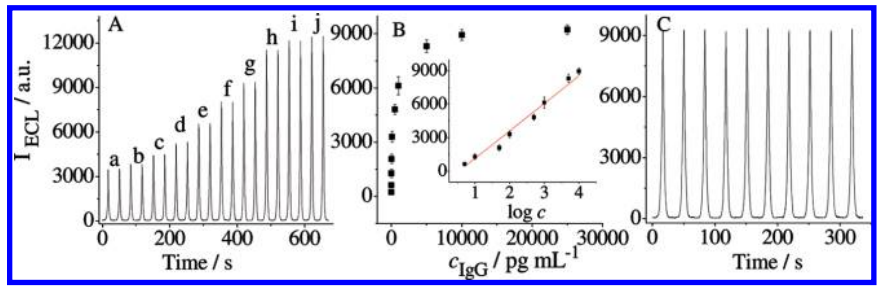

Figure 2. (A) ECL profiles of the immunosensor in the presence of different concentrations of IgG in air-saturated 0.1 M pH 7.4 PBS containing 0.1 M KCl and 0.1 M $K_2S_2O_8$: (a) 1, (b) 5, (c) 10, (d) 50, (e) 100, (f) 500, (g) 1000, (h) 5000, (i) 10 000, (j) 25 000 pg mL^{-1}. (B) Plot of I_{ECL} vs IgG concentration in incubation solution. Inset: linear plot for IgG determination. (C) ECL emission of the immunosensor fabricated using 1 ng mL^{-1} IgG for 10 continuous potential scanning cycles with a scan rate of 100 mV s^{-1} in air-saturated 0.1 M pH 7.4 PBS containing 0.1 M KCl and 0.1 M $K_2S_2O_8$.

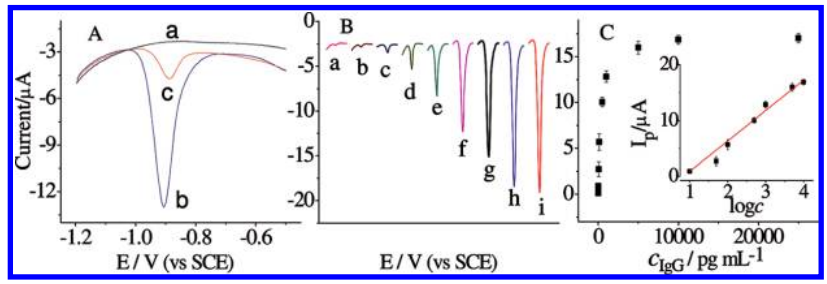

Figure 3. (A) SWV curves recorded after the Ab1−PAB−Au was incubated in 0 (a) and 500 (b and c) pg mL^{-1} IgG solution for 40 min, followed in Si/QD/Ab2 (a and b) and QD/Ab2 (c) for 40 min, and then allowed to dissolve in 0.1 glycine−HCl for 10 min. (B) SWV of Si/QD/Ab2−Ag−Ab1−PAB−Au at IgG concentrations of 1 (a), 5 (b), 10 (c), 50 (d), 100 (e), 500 (f), 1000 (g), 5000 (h), and 10 000 (i) pg mL^{-1}, respectively. (C) Plot of peak current obtained by dissolved Si/QD/Ab2−Ag−Ab1−PAB−Au vs IgG concentration in the incubation solution. Inset in panel C: linear calibration plot.

emission of CdTe QDs immobilized on the Au electrode. The ECL mechanism is illustrated as follows:[3,34]

$$S_2O_8^{2-} + e^- \rightarrow SO_4^{2-} + SO_4^{-\bullet} \quad (1)$$

$$CdTe + e^- \rightarrow CdTe^{-\bullet} \quad (2)$$

$$O_2 + H_2O + 2e^- \rightarrow OOH^- + OH^- \quad (3)$$

$$SO_4^{-\bullet} + CdTe^{-\bullet} \rightarrow CdTe^* + SO_4^{2-} \quad (4)$$

$$2CdTe^{-\bullet} + OOH^- + H_2O \rightarrow 3OH^- + 2CdTe^* \quad (5)$$

$$CdTe^* \rightarrow CdTe + h\nu \quad (6)$$

On the basis of the sandwich immunoassay with Si/QD/Ab2 as the label, an ECL immunosensor was developed for sensitive detection of the target IgG. Figure 2A is the dose−response curve for different IgG concentrations. The ECL intensity increased with increasing IgG concentration in the incubation solution. Figure 2B shows the calibration curve of the Si/QD/Ab2−Ag−Ab1−PAB−Au electrode after deducting background signal. The calibration range of IgG is from 1 pg mL^{-1} to 25 ng mL^{-1}. The linear equation is $I_{ECL} = -1343 + 2468 \log(c/\text{pg mL}^{-1})$ with the correlation coefficient of $R^2 = 0.9766$, where I_{ECL} is the ECL intensity and c is the IgG concentration in the incubation solution. The linear response range of the immunosensor to IgG concentration (inset in Figure 2B) is from 5 pg mL^{-1} to 10 ng mL^{-1}, with a detection limit of 1.3 pg mL^{-1} and a signal-to-noise ratio of 3. Figure 2C shows the ECL emission from the biosensor under continuous potential scanning for 10 cycles. Stable ECL signals were observed, which suggested that the biosensor was suitable for ECL detection.

Signal Amplification Using Si/QD/Ab2 as a Label in SWV Assay. Captured CdTe QDs on gold could be detected by a BFE after dissolving the captured CdTe to Cd^{2+} by immersing Si/QD/Ab2−Ag−Ab1−PAB−Au in a 0.1 M pH 2.2 glycine−HCl solution. This permitted quantification of the attached antigen on Ab1−PAB film by the SWV technique. Figure 3A shows the SWV curves for Ab1−PAB−Au incubated in 0 and 0.5 ng mL^{-1} IgG, followed by being incubated in Si/QD/Ab2 suspension. A well-defined peak for the oxidation of Cd was observed from the Si/QD/Ab2 label at around −0.9 V, whereas no peak was observed for an IgG concentration of 0 ng mL^{-1}. Control experiments using Ab2−Ag−Ab1−PAB−Au without labeling with CdTe QDs or Ab1−PAB−Au incubation in Si/QD/Ab2 were also performed. No detectable signal could be observed in the same potential scan. All these results suggested that the stripping signal for Si/QD/Ab2−Ag−Ab1−PAB−Au was attributed to oxidation of the deposited Cd, dissolved from the captured CdTe QDs by glycine−HCl. It also proved that the attachment of Si/QD/Ab2 labels on gold was due to specific immunoreactions. In addition, the oxidation current of 10.05 μA by the Si/QD/Ab2 label was 5.9 times larger than that of 1.70 μA by the QD/Ab2 label (Figure 3A, curve c) at the same IgG concentration. This also confirmed that signal amplification by the Si/QD/Ab2 label came from the increase of CdTe QDs loading in per immunological event.

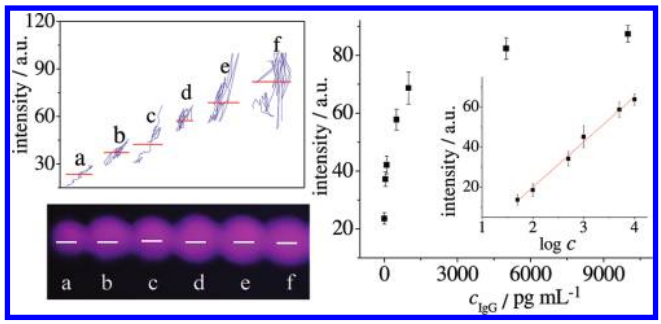

Figure 4. (A) Photo of immunosensors under UV illumination (λ_{ex} = 365 nm) (bottom) and the intensity statistics along the white lines in the photos (top) of samples a−f. The red lines are the average values of intensity. The concentrations of IgG are 0 (a), 50 (b), 100 (c), 500 (d), 1000 (e), and 5000 (f) pg mL^{-1}, respectively. (B) Plot of intensity vs IgG concentration in the incubation solution. Inset in panel B: linear calibration plot.

The oxidation current of Cd was found to be proportional to the concentration of IgG in the incubation solution, within a calibration range from 1 pg mL^{-1} to 25 ng mL^{-1} (Figure 3B, a−i). The linear curve fitted a regression equation of $I_p/\mu A = -4.57 + 5.45 \log(c/\text{pg mL}^{-1})$ in the linear range from 10 pg mL^{-1} to 10 ng mL^{-1} with a correlation coefficient of $R^2 = 0.9938$, where I_p is the oxidation current and c is the IgG concentration in the incubating solution. The lowest detectable concentration of 0.6 pg mL^{-1} at a signal-to-noise ratio of 3 in the present work was much lower than that of the traditional sandwich immunoassay.[49] Our results demonstrated that the proposed methods are highly sensitive, especially for the detection of biomarkers at low levels.

Optical Assay. In addition to ECL and SWV immunoassay, the target IgG on the Au electrode was also detected with optical assay. As mentioned above, in Scheme 2B, QDs on a gold surface are extremely efficient at absorbing UV light and converting it to highly stable fluorescence emission. Figure 4A (bottom) displays photos of a series of immunosensors when using 365 nm as λ_{ex} at IgG concentrations of 0, 50, 100, 500, 1000, and 5000 pg mL^{-1}, respectively. The emission became stronger from left to right, with increasing concentration of IgG. The statistical distribution of the relative emission intensities corresponding to green fluorescence along the white lines was extracted using our self-developed software. These results are plotted in the top of Figure 4A, in which the average intensity is illustrated by red lines. This revealed the relationship (after deducting background signal) between the fluorescence intensity and the IgG concentration, as shown in Figure 4B. The inset in Figure 4B shows a calibration curve, which was suitable for detecting IgG. The fluorescence intensity increased linearly with the IgG concentration within the range frpom 50 pg mL^{-1} to 10 ng mL^{-1}. A detection limit of 12 pg mL^{-1} at a signal-to-noise ratio of 3 was obtained. The linear equation could be represented by $I = -25.19 + 22.57 \log(c/\text{pg mL}^{-1})$ with the correlation coefficient of $R^2 = 0.9917$, where I is the fluorescence intensity and c is the IgG concentration in the incubation solution.

Stability, Precision, Reproducibility, and Regeneration of the Immunosensor. The resultant immunosensor was quite stable. After running for 550 cycles, only a 3% decline of the original ECL was observed for Si/QD/Ab2−Ag−Ab1−PAB−Au (Supporting Information Figure S-5). This demonstrated that the sensing layer of the immunosensor possessed good stability. Reproducibility of the immunosensor for IgG was investigated with intra- and interassay precision. Intraassay precision of the immunosensor was evaluated by assaying one level of IgG for six similar measurements. Interassay precision was estimated by determining one IgG level with six immunosensors made at the same electrode. The intra- and interassay variation coefficients obtained from 1 ng mL^{-1} IgG were 5.1% and 6.7% for ECL assay, 4.7% and 5.9% for SWV assay, and 5.1% and 8.5% for optical assay. Both intra- and interassay of the three applications demonstrated acceptable reproducibility.

The regeneration step was performed using 0.1 mol L^{-1} glycine−HCl (pH 2.2) to interrupt the antigen−antibody immunocomplex. After each sandwich immunoassay, the electrode was immersed in pH 2.2 glycine−HCl for 10 min. No detectable ECL and optical signal could be detected at that moment. Reincubation of this electrode in the IgG-containing solution (1 ng mL^{-1}) followed by incubated in Si/QD/Ab2 suspension resulted in similar ECL and optical responses. Repeating these steps, ECL (Supporting Information Figure S-6), SWV, and fluorescence intensity recovered 97.1%, 94.7%, and 95.8% of the initial value after six assay runs, respectively. This observation also demonstrated that the as-synthesized Si/QD nanospheres possessed good monodispersion and extreme uniformity and were favored as a label for sandwich immunoassay based on ECL, SWV, and optical measurements.

Storage stability of the Si/QD/Ab2−Ag−Ab1−PAB−Au was also investigated by detection of ECL and optical intensities after a sandwich immunoreaction at 1 ng mL^{-1} IgG. No evident decrease in intensity was observed after 3 weeks of storage in 0.01 M PBS at 4 °C, indicating that the prepared immunosensor possessed good storage stability and potential for practical application.

CONCLUSION

With the Si/QD label for signal amplification, two novel versatile immunoassays based on ECL and SWV assays were developed. The goal was to achieve an accurate analysis of samples using a sandwich immunoreaction. A 6.6- and 5.9-fold increase of detection signal was obtained in ECL and SWV assay, respectively, compared with the unamplified method. Optical immunoassay made an excellent complement to ECL and SWV assay to offer a detection result with high accuracy. The immunosensor possessed high sensitivity and good reproducibility and satisfied regeneration and analytical performance. The presented strategy was demonstrated to be simple and specific and could be applied to other biological assays, particularly DNA hybridization.

ACKNOWLEDGMENT

The project is supported by the National Basic Research Program of China (2010CB732400), the National Natural Science Foundation of China (Grant No. 20875013), and the Specialized

(49) Wang, Z. P.; Li, J.; Liu, B.; Li, J. H. *Talanta* **2009**, *77*, 1050–1056.

Research Funds for the Doctoral Program of Higher Education (200802860035).

SUPPORTING INFORMATION AVAILABLE

Characterization of SiO_2, CdTe QDs, Si/QD, and Si/QD/Ab2, SEM images and fluorescence microscopic images of the modified Au substrate, and stability and regeneration of the resultant immunosensor. This material is available free of charge via the Internet at http://pubs.acs.org.

Received for review March 1, 2010. Accepted June 18, 2010.

AC100558T